Chapter 5

Fractional Order Modeling and Control of a Flexible Link Manipulator using Sliding Modes

5.1 Introduction

Effect of fractional controllers has been studied in the previous chapter. The plant model considered was integer order (IO). For an efficient model based control design, it is essential to have a model that can represent the plant more accurately. The dynamics of real systems are often of fractional order (FO) but typically approximated using integer order (IO) models for simplicity. Viscoelasticity seems to be a potential field where the most extensive applications of fractional calculus are found. Viscoelastic materials have their mechanical properties intermediate between those of a pure elastic solid (Hooke model) and a pure viscous fluid (Newton model). Flexibility behaviour lies between solid and viscous behaviour, hence may be treated as a subset of viscoelasticity. To improve the modeling accuracy of flexible link manipulator, fractional model is proposed in this chapter.

Advanced model based control strategy can be developed once an accurate model is available. Most of the references found in literature for control of FLM, have applied FSMC

using fractional surfaces including fractional derivative of the states (PD surface). This necessarily demanded plant to be in the regular form. Therefore such approach was not applicable to systems of multi-state nature.

When the model is fractional, system states also become fractional; which are utilized in the fractional control law. Observer-based control is usually applied when we do not have access to all the states of a system or in an environment where sensors provide noisy output. Therefore fractional observer has to be designed. Fractional states are obtained using a fractional sliding mode observer (FSMO), which are used to implement FSMC.

5.2 Fractional Order Modeling and Control for a Class of Underactuated Systems

SLFM represents a class of underactuated systems which can be represented as follows Any underactuated system can be represented as follows

$$\left.\begin{aligned} \dot{x_1} &= x_3 \\ \dot{x_2} &= x_4 \\ \dot{x_3} &= f_1(\mathbf{x}) + b_1(u) \\ \dot{x_4} &= f_2(\mathbf{x}) + b_2(u) \\ y &= x_1 \end{aligned}\right\} \tag{5.1}$$

where $\mathbf{x}$ is a state vector; $\mathbf{x} = [x_1 \ x_2 \ x_3 \ x_4]^T$ and u is the input. This is an integer order (IO) model.

Now for the same system, a fractional order (FO) model is proposed. As per the fractional theory, the order of differintegrations (differentiation or integration) may not be integer but a fraction lying between two integers [133]. Fractional order differentiations are proposed in the dynamic equations of the system described in (5.1). The fractional order model for the above

system is proposed as

$$\left.\begin{aligned} D^{\beta}x_1 &= x_3 \\ D^{\beta}x_2 &= x_4 \\ D^{\zeta}x_3 &= f_1(\mathbf{x}) + b_1 u \\ D^{\zeta}x_4 &= f_2(\mathbf{x}) + b_2 u \\ y &= x_1, \end{aligned}\right\} \tag{5.2}$$

where ζ and β are any fractional number lying between 0 and 1. D denotes differentiation operator. Fractional orders in the model need not be same for each of x_i for $i = 1$ to 4. We have chosen two fractional orders namely ζ and β for fractional model description. Order β is considered for first two fractional differential equations and ζ for the remaining two equations. In fractional calculus, if the orders of these differential equations are same for a particular model, then the order of the plant model is said to be commensurate [133]. If the orders are different, then the model is said to be a non-commensurate order model. Since different fractional orders are used for describing the dynamic equation of the underactuated system, it is a non-commensurate fractional order system. The non linear system (5.2) can be represented by linear uncertain system [134] as shown below,

$$\left.\begin{aligned} D^{fr}\mathbf{x} &= A\mathbf{x} + \mathbf{b}u + \mathbf{d} \\ y &= \mathbf{cx} \end{aligned}\right\} \tag{5.3}$$

where fr denotes fractionality, $A \in \mathbb{R}^{4\times4}$, input matrix $\mathbf{b} \in \mathbb{R}^{4\times1}$ and $\mathbf{c} \in \mathbb{R}^{1\times4}$ is the output matrix. $A\mathbf{x} + \mathbf{b}u$ represents linear part and **d** represents the lumped nonlinearities, uncertainties and disturbances of the system. Representing (5.2) in this manner we get,

$$\begin{aligned} A &= \begin{bmatrix} 0 & 0 & 1 & 0 \\ 0 & 0 & 0 & 1 \\ a_1 & a_2 & a_3 & a_4 \\ a_5 & a_6 & a_7 & a_8 \end{bmatrix}, \mathbf{b} = \begin{bmatrix} 0 \\ 0 \\ b_1 \\ b_2 \end{bmatrix}, \\ \mathbf{d} &= \begin{bmatrix} 0 & 0 & d_1 & d_2 \end{bmatrix}^T, \mathbf{c} = \begin{bmatrix} 1 & 0 & 0 & 0 \end{bmatrix} \end{aligned}$$

where $a_i, (i = 1 \text{ to } 8), b_1, b_2$ are parameters of system matrix.

Defining $\mathbf{z}_1 \equiv [x_1 \ x_2]^T$ and $\mathbf{z}_2 \equiv [x_3 \ x_4]^T$, the proposed model (5.3) can be written as,

$$\left.\begin{aligned} D^{\beta}\mathbf{z}_1 &= \mathbf{z}_2 \\ D^{\zeta}\mathbf{z}_2 &= A_{21}\mathbf{z}_1 + A_{22}\mathbf{z}_2 + B_2 u + \bar{\mathbf{d}} \\ y &= \mathbf{cx} \end{aligned}\right\} \tag{5.4}$$

$$\begin{aligned} A_{21} &= \begin{bmatrix} a_1 & a_2 \\ a_5 & a_6 \end{bmatrix}, A_{22} = \begin{bmatrix} a_3 & a_4 \\ a_7 & a_8 \end{bmatrix}, \\ B_2 &= \begin{bmatrix} \bar{b}_1 & \bar{b}_2 \end{bmatrix}^T, \bar{\mathbf{d}} = \begin{bmatrix} \bar{d}_1 & \bar{d}_2 \end{bmatrix}^{\mathbf{T}} \end{aligned}$$

For this fractional order model, fractional order controller-observer scheme is proposed in sliding mode as follows.

5.3 Fractional Order Sliding Mode Control (FSMC)

Design of fractional order sliding mode control consists of two steps; design of stable sliding surface and synthesis of control law to ensure existence of sliding modes. The proposed sliding surface, control synthesis and detailed stability proof is described in the following subsections.

5.3.1 Fractional sliding surface

Initially, for an integer order system, a stable sliding surface is

$$s = \mathbf{c}^T\mathbf{x}$$

Here $\mathbf{c}^T = [c_1 \ c_2 \ c_3 \ c_4] \in \mathbb{R}^{1\times 4}$ is a sliding surface matrix. It may be noted that the same sliding surface matrix parameters designed for integer order system are used while devising the proposed fractional sliding surface. For the fractional system, a novel fractional sliding surface is proposed and is given as,

$$s_f = r_1\mathbf{c}_2\mathbf{z}_2 + r_2\mathbf{c}_2 I^{\zeta}\mathbf{z}_2 + r_3\mathbf{c}_1 D^{\beta-\zeta}\mathbf{z}_1 \tag{5.5}$$

where

$$\mathbf{c}_1 = [c_1 \;\; c_2]$$

and

$$\mathbf{c}_2 = [c_3 \;\; c_4]$$

are all positive constants. The three tuning parameters r_1, r_2 and r_3 give more freedom to adjust the tuning of the required performance indices.

Fractional order derivatives are defined from Caputo's definition of fractional derivative.

5.3.2 Synthesis of Fractional Control Law

A reaching law in fractional domain as proposed in [135] is,

$$D^{\zeta} s_f = -k\text{sgn}s_f - qs_f, \tag{5.6}$$

where k, $q > 0$ are tuning parameters.

For designing control, differentiate (5.5) with fractional order ζ,

$$D^{\zeta} s_f = r_1 \mathbf{c}_2 D^{\zeta} \mathbf{z}_2 + r_2 \mathbf{c}_2 \mathbf{z}_2 + r_3 \mathbf{c}_1 D^{\beta} \mathbf{z}_1 \tag{5.7}$$

Substituting for $D^{\zeta} z_2$ from(5.4),

$$D^{\zeta} s_f = r_1 \mathbf{c}_2 (A_{21}\mathbf{z}_1 + A_{22}\mathbf{z}_2 + B_2 u + \bar{\mathbf{d}}) + r_2 \mathbf{c}_2 \mathbf{z}_2 + r_3 \mathbf{c}_1 \mathbf{z}_2 \tag{5.8}$$

Equating (5.6) and (5.8)

$$-k\text{sgn}s_f - qs_f = r_1 \mathbf{c}_2 (A_{21}\mathbf{z}_1 + A_{22}\mathbf{z}_2 + B_2 u + \bar{\mathbf{d}}) + r_2 \mathbf{c}_2 \mathbf{z}_2 + r_3 \mathbf{c}_1 \mathbf{z}_2 \tag{5.9}$$

Control is obtained as

$$\begin{aligned} u_{fsmc} &= (r_1 \mathbf{c}_2 B_2)^{-1} [-k\text{sgn}s_f - qs_f - r_1 \mathbf{c}_2 A_{21} \mathbf{z}_1 \\ &- (r_2 \mathbf{c}_2 + r_3 \mathbf{c}_1 + r_1 \mathbf{c}_2 A_{22}) \mathbf{z}_2 - r_1 \mathbf{c}_2 \bar{\mathbf{d}}] \end{aligned}$$

This control is not feasible as the disturbance term is unknown. Hence, the implementable control is considered;

$$\begin{aligned} u_{fsmc} &= (r_1 \mathbf{c}_2 B_2)^{-1} [-k\text{sgn}s - qs - r_1 \mathbf{c}_2 A_{21} \mathbf{z}_1 \\ &- (r_2 \mathbf{c}_2 + r_3 \mathbf{c}_1 + r_1 \mathbf{c}_2 A_{22}) \mathbf{z}_2] \end{aligned} \tag{5.10}$$

This is the necessary FSMC.

5.3.3 Existence of Sliding

Finite time reaching to the proposed fractional surface in (5.5) is proved using Lyapunov approach.

Consider a candidate Lyapunov function $V(s_f) = {s_f}^2$.

Its ζ^{th} derivative is given as per Leibniz rule of fractional differentiation as follows

$$\frac{d^\zeta V}{dt^\zeta} = D^\zeta V = s_f D^\zeta s_f + P_s, \tag{5.11}$$

where

$$P_s = \sum_{k=1}^{\infty} \frac{\Gamma(1+\zeta)}{\Gamma(1+k)\Gamma(1-k+\zeta)} D^k s_f D^{\zeta-k} s_f.$$

It is assumed that the following inequality holds [136]

$$|P_s| \leq N|s_f|$$

where N is a positive number. Substituting $D^\zeta s$ from (5.7) in (5.11),

$$D^\zeta V = s_f(r_1 \mathbf{c}_2 D^\zeta \mathbf{z}_2 + r_2 \mathbf{c}_2 \mathbf{z}_2 + r_3 \mathbf{c}_1 \mathbf{z}_2) + N|s_f|$$

Using the system dynamics (5.4),

$$D^\zeta V = s_f(r_1 \mathbf{c}_2(A_{21}\mathbf{z}_1 + A_{22}\mathbf{z}_2 + B_2 u + \bar{\mathbf{d}}) + r_2 \mathbf{c}_2 \mathbf{z}_2 + r_3 \mathbf{c}_1 \mathbf{z}_2) + N|s_f|$$

substituting the value of control input from (5.10),

$$\begin{aligned} D^\zeta V &= s_f(-k\text{sgn}(s_f) - q s_f + r_1 \mathbf{c}_2 D) + N|s_f| \\ &= -k|s_f| - q(s_f)^2 + |s_f| r_1 \mathbf{c}_2 D + N|s_f| \\ &\leq -|s_f|(k - r_1 \mathbf{c}_2 D - N) - q(s_f)^2. \end{aligned}$$

If $k > |r_1 \mathbf{c_2 D_{max}} + \mathbf{N}|$, $D^\zeta(V)$ becomes negative definite.

Thus with this choice of k, finite time convergence of the surface and hence the existence of the sliding mode is guaranteed.

5.3.4 Stability Analysis of Fractional Sliding Surface

Reachability condition for the proposed fractional surface is proved above. Stability of the fractional surface (5.5) is is also a necessary condition to be satisfied. The fractional order

system described in (5.4) is constrained to the sliding surface (5.5) during sliding mode i.e. $s_f = 0$.

Therefore from (5.5)

$$r_1\mathbf{c}_2\mathbf{z}_2 + r_2\mathbf{c}_2 I^{\zeta}\mathbf{z}_2 + r_3\mathbf{c}_1 D^{\beta-\zeta}\mathbf{z}_1 = 0$$

From system dynamics (5.4)

$$r_1\mathbf{c}_2 D^{\beta}\mathbf{z}_1 + r_2\mathbf{c}_2 D^{\beta-\zeta}\mathbf{z}_1 + r_3\mathbf{c}_1 D^{\beta-\zeta}\mathbf{z}_1 = 0$$

$$r_1\mathbf{c}_2 D^{\beta}\mathbf{z}_1 + (r_2\mathbf{c}_2 + r_3\mathbf{c}_1) D^{\beta-\zeta}\mathbf{z}_1 = 0$$

Therefore $D^{\beta}\mathbf{z}_1$ becomes

$$\begin{aligned} D^{\beta}\mathbf{z}_1 &= -\frac{r_2\mathbf{c}_2 + r_3\mathbf{c}_1}{r_1\mathbf{c}_2 + r_2\mathbf{c}_2 + r_3\mathbf{c}_1} I^{\zeta}\mathbf{z}_1 \\ &= -aI^{\zeta}\mathbf{z}_1 \end{aligned} \tag{5.12}$$

where

$$a = \frac{r_2\mathbf{c}_2 + r_3\mathbf{c}_1}{r_1\mathbf{c}_2 + r_2\mathbf{c}_2 + r_3\mathbf{c}_1}$$

Theorem: The proposed fractional sliding surface given in (5.5) is stable if $a > 0$.

Proof: According to Fractional order extension of Lyapunov direct method [137], if fractional derivative of a valid Lyapunov function is negative definite then the states of fractional system converge asymptotically.

Consider a candidate Lyapunov function, $V(\mathbf{z}_1) = \mathbf{z}_1^T P\mathbf{z}_1$, where P is a positive definite matrix taken as identity matrix of order 2.

Taking its β^{th} derivative of the Lyapunov function and using (5.12),

$$D^{\beta}V(\mathbf{z}_1) = D^{\beta}\mathbf{z}_1^T(P\mathbf{z}_1) + \mathbf{z}_1^T P D^{\beta}\mathbf{z}_1$$

Substituting for $D^{\beta}z_1$, to get

$$D^{\beta}V(\mathbf{z}_1) = -I^{\zeta}\mathbf{z}_1(a)P\mathbf{z}_1 + \mathbf{z}_1^T P(-I^{\zeta}\mathbf{z}_1 a)$$

$$\begin{aligned} D^{\beta}V(\mathbf{z}_1) &= I^{\zeta}(\mathbf{z}_1^T(-aP - Pa)\mathbf{z}_1) \\ &= -I^{\zeta}(\mathbf{z}_1^T \begin{bmatrix} 2a & 0 \\ 0 & 2a \end{bmatrix} \mathbf{z}_1) \\ &= -I^{\zeta}(\mathbf{z}_1^T Q\mathbf{z}_1) \end{aligned}$$

where

$$Q = \begin{bmatrix} 2a & 0 \\ 0 & 2a \end{bmatrix}$$

Taking ζ^{th} derivative

$$\begin{aligned} D^{\beta+\zeta}V(\mathbf{z}_1) &= -(\mathbf{z}_1^T Q \mathbf{z}_1) \\ \Rightarrow D^{\gamma}V(\mathbf{z}_1) &= -\mathbf{z}_1^T Q \mathbf{z}_1 \end{aligned}$$

where $\gamma = \beta + \zeta$. For Q to be positive definite, $a > 0$. γ may take a value from 0 to 2. In [123], stability of the fractional Lyapunov function is proved for fractional order $0 \leq \gamma < 1$, and extended in [124] for fractional order $1 \leq \gamma < 2$.
This completes the proof.

It is observed that to implement control law (5.10), complete state vector is required. The states evolved from the fractional order model are also fractional, which can not be obtained using sensors or estimated using conventional observer. Therefore a fractional state observer is required, which will be able to provide the state vector from the knowledge of system output only. In the following section, a fractional order sliding mode observer (FSMO) is proposed.

5.4 Fractional Order Sliding Mode Observer

State estimation requires knowledge of the plant, the control input and the sensor signal. Observers provide the important advantage of complete or partial removal of sensors, which reduces cost and improves reliability.
In this study, FSMO is developed for the proposed FO system (5.3).

5.4.1 Observer Design

For designing the observer, nominal plant is considered. Transforming the system using $\mathbf{w} \leftrightarrow T_c\mathbf{x}$, so as to get $C = [0 \ \ I_p]$, where I_p is the identity matrix of order 1, the transformed system

is written as,

$$\left.\begin{aligned} D^{fr}\mathbf{w} &= A_{reg_o}\mathbf{w} + B_{reg_o}u \\ y &= \begin{bmatrix} 0 & 0 & 0 & 1 \end{bmatrix}\mathbf{w}. \end{aligned}\right\} \tag{5.13}$$

The state vector **w** is partitioned as $[\mathbf{w}_1 \;\; \mathbf{w}_2]^T$ where

$\mathbf{w}_1 = \begin{bmatrix} w_{11} & w_{12} & w_{13} \end{bmatrix}^T$ and $\mathbf{w}_2 = w_2$.

From the output equation, we get, $y = w_2$.

The fractional derivative state vector is given as $D^{fr}\mathbf{w} \equiv \begin{bmatrix} D^{\beta}w_{11} & D^{\zeta}w_{12} & D^{\zeta}w_{13} & D^{\beta}w_2 \end{bmatrix}^T$

The partitioned state and input matrices are,

$A_{reg_o} = \begin{bmatrix} \bar{A}_{11} & \bar{A}_{12} \\ \bar{A}_{21} & \bar{A}_{22} \end{bmatrix}$ and $B_{reg_o} = \begin{bmatrix} \bar{B}_1 \\ \bar{B}_2 \end{bmatrix}$,

where $\bar{A}_{11} = \begin{bmatrix} 0 & 0 & 1 \\ a_2 & a_3 & a_4 \\ a_6 & a_7 & a_8 \end{bmatrix}$; $\bar{A}_{12} = \begin{bmatrix} 0 \\ a_1 \\ a_5 \end{bmatrix}$; $\bar{A}_{21} = \begin{bmatrix} 0 & 1 & 0 \end{bmatrix}$ and $A_{22} = 0$

$\bar{B}_1 = \begin{bmatrix} 0 & b_1 & b_2 \end{bmatrix}^T$; $\bar{B}_2 = 0$.

The transformed dynamics are written as,

$$\left.\begin{aligned} D^{fr}\mathbf{w}_1 &= \bar{A}_{11}\mathbf{w}_1 + \bar{A}_{12}y + \bar{B}_1 u \\ D^{\beta}y &= \bar{A}_{21}\mathbf{w}_1 + \bar{A}_{22}y + \bar{B}_2 u. \end{aligned}\right\} \tag{5.14}$$

Defining the observer sliding surface as

$$s = y - \hat{y} = e_y$$

FSMO proposed is,

$$\left.\begin{aligned} D^{fr}\hat{\mathbf{w}}_1 &= \bar{A}_{11}\hat{\mathbf{w}}_1 + \bar{A}_{12}\hat{y} + \bar{B}_1 u + L\nu \\ D^{\beta}\hat{y} &= \bar{A}_{21}\hat{\mathbf{w}}_1 + \bar{A}_{22}\hat{y} + \bar{B}_2 u + \nu. \end{aligned}\right\} \tag{5.15}$$

$L \in \mathbb{R}^{3\times 1}$ is the observer gain matrix. The error function is $\nu = k_o \text{sgn}(e_y)$. The positive scalar k_o is the tuning parameter chosen to ensure the existence of sliding. The error dynamics can be written from (5.14) and (5.15) as follows;

$$\begin{aligned} D^{fr}\mathbf{e}_{w1} &= \bar{A}_{11}\mathbf{e}_{w1} + \bar{A}_{12}e_y - L\nu \\ D^{\beta}e_y &= \bar{A}_{21}\mathbf{e}_{w1} + \bar{A}_{22}e_y - \nu \end{aligned} \tag{5.16}$$

where, $e_{w11} = w_{11} - \hat{w}_{11}, e_{w12} = w_{12} - \hat{w}_{12}, e_{w13} = w_{13} - \hat{w}_{13}$ and $e_y = y - \hat{y}$.

The error vector is, $\mathbf{e}_{w1} = \begin{bmatrix} e_{w11} & e_{w12} & e_{w13} \end{bmatrix}^T$.

During sliding, $s = 0 \Rightarrow e_y = 0$ and hence $D^{\beta} e_y = 0$, therefore (5.16) becomes;

$$D^{fr}\mathbf{e}_{w1} = (\bar{A}_{11} - L\bar{A}_{21})\mathbf{e}_{w1} \tag{5.17}$$

If λ_i are the eigenvalues of $(\bar{A}_{11} - L\bar{A}_{21})$, the poles of the fractional error dynamics in (5.17) are $pi = \lambda_i^{1/fr}$. This solution will suffice for non-commensurate system, as it can be broken down to ζ and β parameters. Thus, stability is attained if poles lie in the negative half of s-plane i.e. if $|arg(pi) > \pi/2|$. This stability condition holds for non-commensurate system. Thus, L is designed to ensure $(\bar{A}_{11} - L\bar{A}_{21})$ to be stable.

5.4.2 Stability Analysis for FSMO

The error dynamics of FSMO is given in (5.16). The stability of this equation is proved here. Consider a Lyapunov candidate function $V(e_y) = e_y^2$. The β^{th} derivative of $V(e_y)$ is taken according to (5.11).

$$\begin{aligned}
(D^{\beta} e_y)e_y &= (\bar{A}_{21}\mathbf{e}_{w1} - \nu)e_y \\
&= \bar{A}_{21}\mathbf{e}_{w1}e_y - k_o sgn(e_y)e_y \\
&= \bar{A}_{21}\mathbf{e}_{w1}e_y - k_o|e_y| \\
&\leq -|e_y|(k_o - |\bar{A}_{21}\mathbf{e}_{w1}|).
\end{aligned}$$

So, if $k_o > |\bar{A}_{21}\mathbf{e}w1| + \eta$, where η is a small positive constant, $D^{\beta} e_y e_y \leq \eta|e_y|$ is ascertained. Using this last inequality with the boundary condition;

$$\begin{aligned}
D^{\beta}V &\leq -|e_y|(k_o - |\bar{A}_{21}\mathbf{e}_{w1}|) + P \\
D^{\beta}V &\leq -|e_y|(k_o - |\bar{A}_{21}\mathbf{e}_{w1}|) + N_2|e_y| \\
D^{\beta}V &\leq -|e_y|(k_o - |\bar{A}_{21}\mathbf{e}_{w1} - N_2|)
\end{aligned}$$

Thus, if $k_o > |A_{21}\mathbf{e}_{w1} + N_2| + \eta$; the condition $D^{\beta}V \leq \eta|e_y|$ is verified. This ensures finite time convergence of the output estimation error to zero and the remaining states converge asymptotically by the virtue of the design.

SLFM is an underactuated system. Proposed fractional sliding mode controller-observer theory is applied to SLFM and explained in the next section.

5.5 Fractional Order Model of SLFM

Integer order model of SLFM is given in (2.21). Accounting for uncertainties and matched disturbances, the dynamics is written as

$$\left.\begin{aligned} \dot{\mathbf{x}} &= A\mathbf{x} + \mathbf{b}u + \mathbf{d} \\ y &= \mathbf{cx} \end{aligned}\right\} \tag{5.18}$$

With system matrices given in Chapter 2 Section 2.3, proposed fractional model for SLFM based on (5.3) is,

$$\left.\begin{aligned} D^{\beta}\mathbf{z}_1 &= \mathbf{z}_2 \\ D^{\zeta}\mathbf{z}_2 &= A_{21}\mathbf{z}_1 + A_{22}\mathbf{z}_2 + B_2 u + \bar{\mathbf{d}} \\ y &= \mathbf{cx} \end{aligned}\right\}$$

where

$$\begin{aligned} A_{21} &= \begin{bmatrix} 0 & 212.7 \\ 0 & -616.9 \end{bmatrix}, A_{22} = \begin{bmatrix} -19.65 & 0 \\ 19.65 & 0 \end{bmatrix}, \\ B_2 &= \begin{bmatrix} 34.6 & -34.6 \end{bmatrix}^T \end{aligned}$$

To check the correctness of this model, it has to be validated using experimentation results of actual plant.

5.5.1 Model Validation

For any physical dynamic system, model validation is done by comparing the simulation results of the mathematical model with experimental results. The plant under consideration is shown in Chapter 2 Figure 2.3. Model validation is performed as described below. For the given plant we have considered two models Integer order (IO) and Fractional Order (FO). In fact no model is perfect. Both IO and FO models are approximate representations of the plant. IO model reported in the literature and proposed FO model were simulated.

mbox The plant was excited by square wave input with frequency 1.5 Hz and amplitude 0.1. Then vibrations of the link were noted. For comparison, same excitation was given to the models (FO and IO) in simulation and the outputs were obtained. The tip displacement results from both the simulated models and from the actual plant are shown in Figure 5.1.

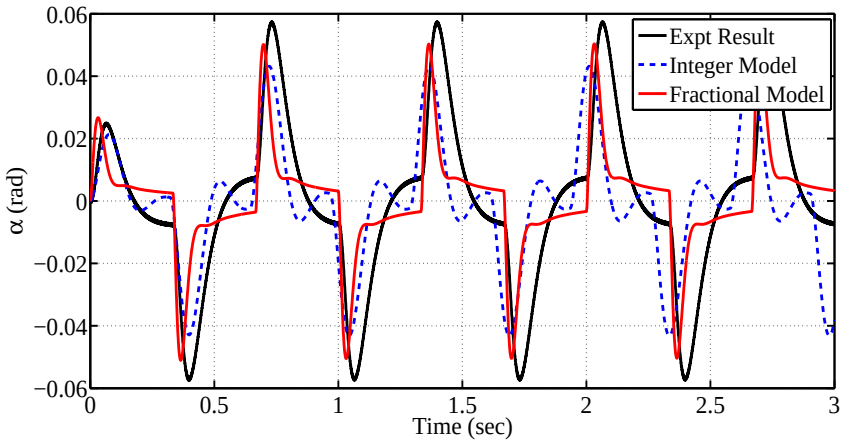

Figure 5.1: Tip deflection for simulation models (FO and IO) and for actual plant

The outputs from plant and simulated models (IO and FO) were compared and modeling errors were obtained. The errors evaluate the degree of accuracy of the models. The plot of the modeling errors is shown in Figure 5.2.

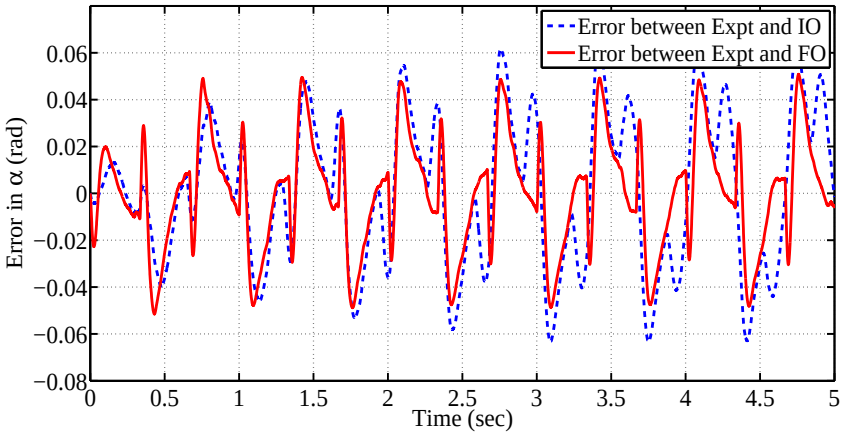

Figure 5.2: Modeling errors

To quantify model accuracies, norm 1 of the errors between plant output and model output were obtained for each of the models (IO and FO). It was found that this error norm for IO model was 257.76 and for FO model was 143.24. It is very obvious that lesser the 1 norm of error, better is the corresponding model. Since 1 norm of model error of FO model is about 44% less than that of the IO model, we concluded that FO model is better than IO model.

Orders of the fractional model are fixed in a non-commensurate manner to get this minimized error. During this experimentation, the values of ζ and β were obtained as β=0.92, ζ=0.71. It is observed that the non commensurate FO model is more closer to the actual plant. For this plant fractional order control and estimation is designed. The proposed fractional scheme including model, controller and observer is verified in simulation and to show its effectiveness is compared with an integer model, control and observer. For the integer model (5.1) developed in Chapter 2 controller and observer using sliding mode is developed.

5.5.2 Integer Order Controller and Observer for SLFM

The sliding mode control is synthesized using surface s designed in Chapter 3 Section 3.5.1. Differentiating the same

$$\dot{s} = \mathbf{c}^T \dot{\mathbf{x}}$$

Substituting $\dot{\mathbf{x}}$ from system dynamics

$$\dot{s} = \mathbf{c}^T (Ax + \mathbf{b}u) \tag{5.19}$$

Gao's constant plus proportional reaching law is

$$\dot{s} = -ksgn(s) - qs, \tag{5.20}$$

where $k > 0$ and $q > 0$ are the tuning parameters. Using (5.20) in (5.19), the control law becomes

$$u_{(SMC)} = (\mathbf{c}^T \mathbf{b})^{-1} (-\mathbf{c}^T A\mathbf{x} - ksgn(s) - qs) \tag{5.21}$$

Approximate tuning of the parameters renders a stable performance of the system.
Sliding matrix $\mathbf{c}^T$ is $[5 \quad -24.3847 \;\; 1.0291 \quad -0.3851]$.
The state vector for this control is obtained from a SMO designed for the integer order counterpart of system representation (5.13). The SMO is as follows

$$\left.\begin{aligned} \dot{\hat{\mathbf{w}}}_1 &= \bar{A}_{11}\hat{\mathbf{w}}_1 + \bar{A}_{12}\hat{y} + \bar{B}_1 u + L\nu \\ \dot{\hat{y}} &= \bar{A}_{21}\hat{\mathbf{w}}_1 + \bar{A}_{22}\hat{y} + \bar{B}_2 u + \nu. \end{aligned}\right\} \tag{5.22}$$

with

$$\begin{aligned}\dot{\mathbf{w}}_1 &= \begin{bmatrix} 0 & 0 & 1 \\ 936.93 & -41.19 & 0 \\ -1372.6 & 41.19 & 0 \end{bmatrix} \mathbf{w}_1 + \begin{bmatrix} 0 \\ 0 \\ 0 \end{bmatrix} \hat{y} \\ &+ \begin{bmatrix} 0 \\ 72.4593 \\ -72.4593 \end{bmatrix} u + L\nu \\ \dot{y} &= \begin{bmatrix} 0 & 1 & 0 \end{bmatrix} \mathbf{w}_1 + 0\hat{y} + 0u + \nu. \end{aligned} \tag{5.23}$$

The observer gain matrix is $L = [0.4052\ 31.8100\ -51.0150]^T$ to have observer poles at $[-18\ , -20\ , -25]$ and $k_o = 5.7$.

5.5.3 Fractional Controller and Observer for SLFM

FSMC proposed in Section 5.3 is developed for SLFM. Fractional surface proposed for SLFM is

$$s_f = r_1\mathbf{c}_2\mathbf{z}_2 + r_2\mathbf{c}_2 I^{\zeta}\mathbf{z}_2 + r_3\mathbf{c}_1 D^{\beta-\zeta}\mathbf{z}_1$$

with the control law

$$\begin{aligned} u_{fsmc} &= (r_1\mathbf{c}_2 B_2)^{-1}[-k\text{sgn}s_f - qs_f - r_1\mathbf{c}_2 A_{21}\mathbf{z}_1 \\ &- (r_2\mathbf{c}_2 + r_3\mathbf{c}_1 + r_1\mathbf{c}_2 A_{22})\mathbf{z}_2] \end{aligned} \tag{5.24}$$

For SLFM from sliding surface matrix, $\mathbf{c}_1 = [5\ -24.3847]$, $\mathbf{c}_2 = [1.0291\ -0.3851]$

The tuning parameters are r_1=0.45; r_2=0.55; r_3=0.001;

Fractional orders are β=0.92, ζ=0.71

FSMO for this plant is developed as described in (5.15), and is given as,

$$\left.\begin{aligned}\begin{bmatrix} D^{\beta}\hat{w}_{11} \\ D^{\zeta}\hat{w}_{12} \\ D^{\zeta}\hat{w}_{13} \end{bmatrix} &= \begin{bmatrix} 0 & 0 & 1 \\ 936.93 & -41.19 & 0 \\ -1372.6 & 41.19 & 0 \end{bmatrix} \begin{bmatrix} \hat{w}_{11} \\ \hat{w}_{12} \\ \hat{w}_{13} \end{bmatrix} \\ &+ \begin{bmatrix} 0 \\ 0 \\ 0 \end{bmatrix} \hat{y} + \begin{bmatrix} 0 \\ 72.4593 \\ -72.4593 \end{bmatrix} u + L\nu \\ D^{\zeta}\hat{y} &= \begin{bmatrix} 0 & 1 & 0 \end{bmatrix} \begin{bmatrix} \hat{w}_{11} \\ \hat{w}_{12} \\ \hat{w}_{13} \end{bmatrix} + 0\hat{y} + 0u + \nu. \end{aligned}\right\} \tag{5.25}$$

$L \in \mathbb{R}^{3\times 1}$ is the observer gain matrix and $\nu = k_o sgn(y - \hat{y})$. The observer gain matrix is found to have the value $L = [5.83 \ 102.81 \ -55.61]^T$ and $k_o = 5.7$ for this fractional SMO. The observer pole locations were designed at [-21 -22 -30].

5.6 Simulation Results

Performance of conventional SMC (5.21) with states reconstructed using SMO (5.23) is compared with that of fractional SMC (5.24) and fractional SMO (5.25). The SLFM was simulated to track a angular displacement of 15° at 0.5 sec time delay. The system is analyzed with $\pm 10\%$ parametric variations.

The desired performance specifications were: Settling time T_s= 1.5 seconds and percentage overshoot $<$ 10%.

SMC was tuned to get the the desired performance with gains $k = 5.5, q = 3.6$.

FSMC was also tuned to yield the desired performance. For FSMC Controller gains were $k = 2.2$; $q = 1.8$.

5.6.1 Performance of SMO and FSMO

For the designed integer order SMO (5.23) performance is analyzed by plotting the estimation errors. Figure 5.3 shows the estimation error for angular displacement and its velocity. The estimation errors of α and $\dot{\alpha}$ are shown in Figure 5.4

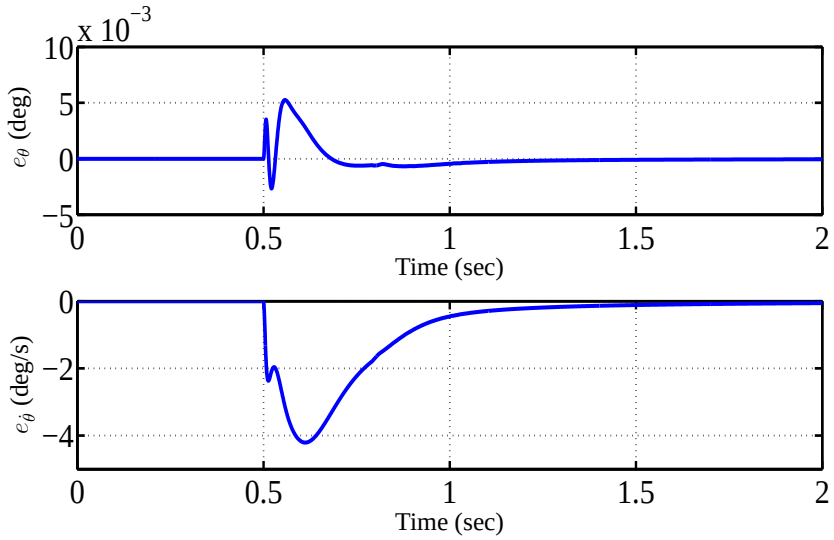

Figure 5.3: SMO:Estimation error in θ and $\dot{\theta}$

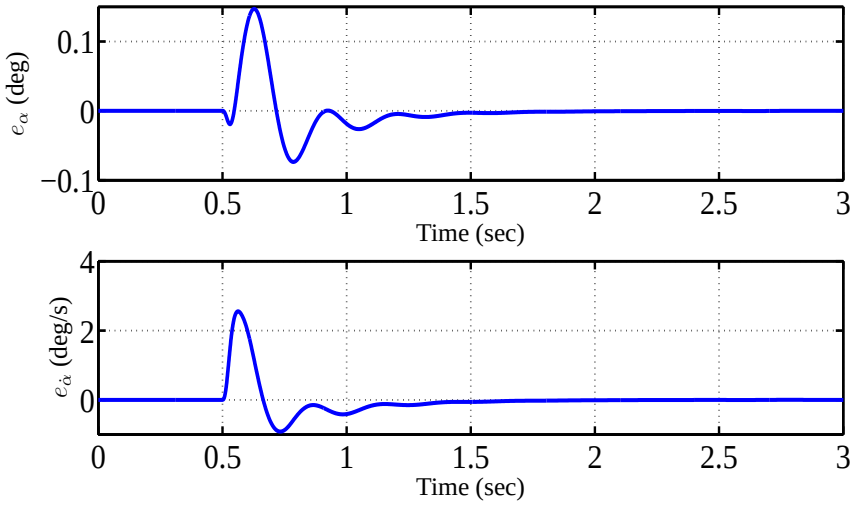

Figure 5.4: SMO:Estimation error in α and $\dot{\alpha}$

For the designed FSMO (5.25) performance is analyzed by plotting the estimation errors. Figure 5.5 and 5.6 show the estimation error for all of the states.

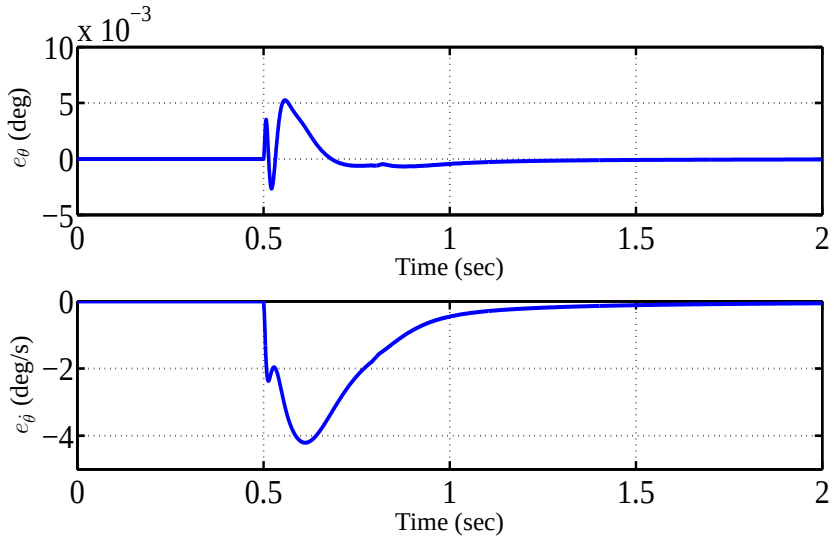

Figure 5.5: FSMO: Estimation error in θ and $\dot{\theta}$

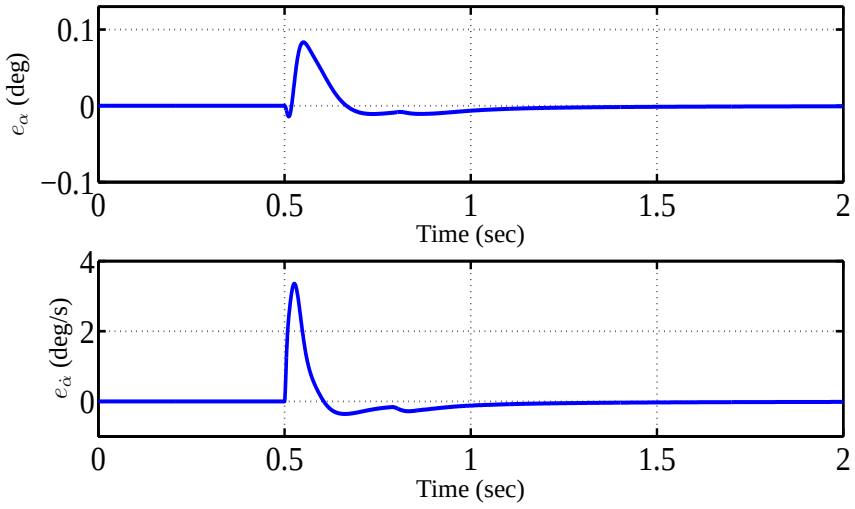

Figure 5.6: FSMO: Estimation error in α and $\dot{\alpha}$

It can be observed from the estimation error plots that output estimation error converges to zero in finite time in both SMO and FSMO. Estimation error convergence time in the remaining states in FSMO is 50% lesser than that of SMO.

5.6.2 Performance: FSMC with FSMO and SMC with SMO

Performance of SMC with SMO for integer order plant and performance of FSMC with FSMO for the proposed fractional SLFM plant were compared in simulation. A step command of 15° was applied. Figure 5.7 shows the evolution of angular displacement of the link with its velocity. Figure 5.8 shows the plot of tip displacement and its rate. Plot of the control input to the system is shown in Figure 5.9.

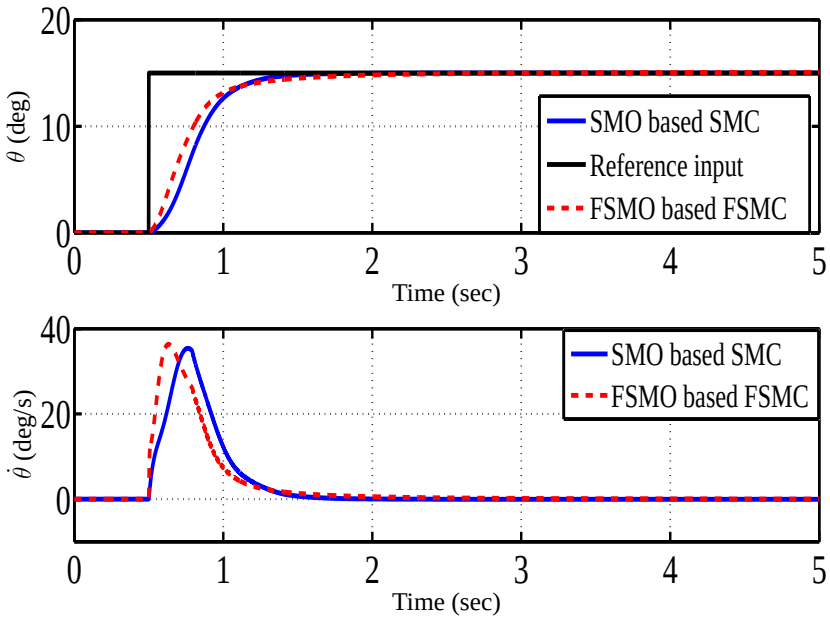

Figure 5.7: Angular displacement and its rate of change

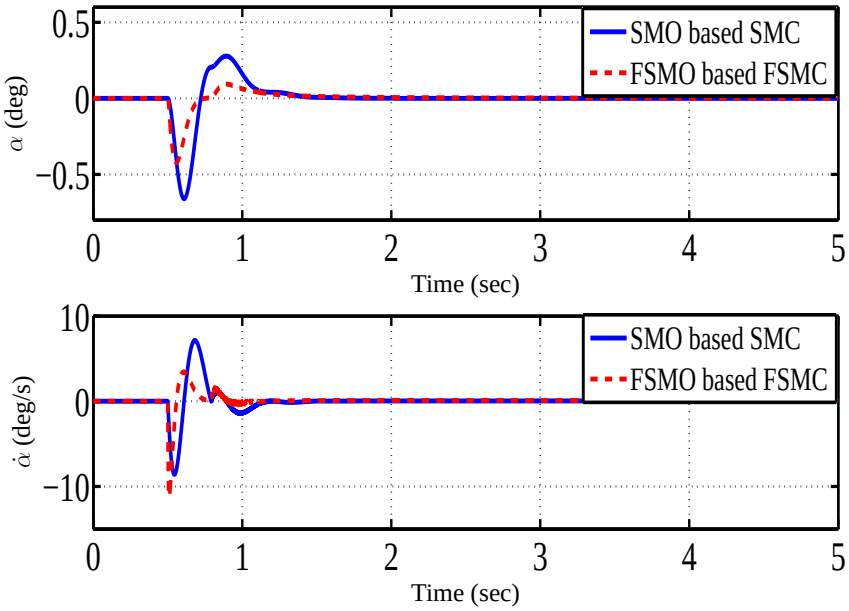

Figure 5.8: Tip displacement and its rate of change

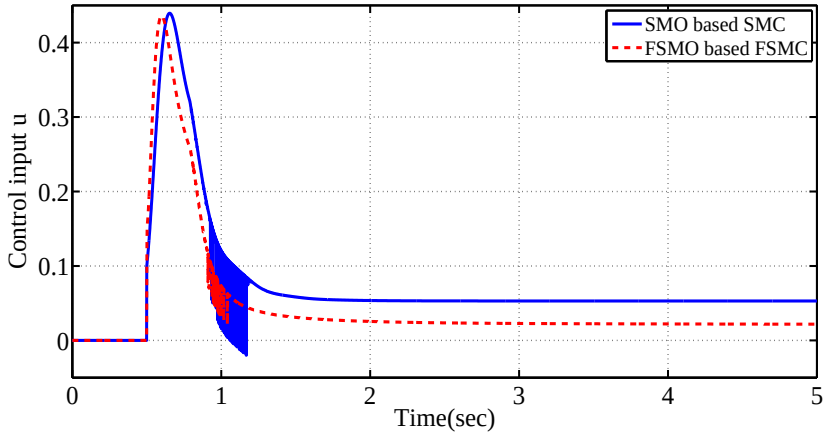

Figure 5.9: Control input

It can be seen from the simulation plots that for similar output performance in terms of settling time, FSMC with FSMO results show reduced vibrations and reduced control efforts. 1-norm of the tip vibration is a measure of tip control quality. Tip vibrations are seen to be reduced by around 24% using FSMC with FSMO scheme compared to SMC with SMO. Also the control efforts are reduced by 10%. The qualitative analysis is tabulated in Table 5.1.

Strategy	$\|u\|_2$	$\|u\|_\infty$	$\|\theta\|_1$	$\|\alpha\|_1$
SMC with SMO	7.76	0.44	62064	164.45
FSMC with FSMO	6.5	0.43	62195	124.26

Table 5.1: Comparison of performance for SMC and FSMC in simulation

5.7 Experimental Results

SMC with SMO and FSMC with FSMO in (5.21) and (5.24) were implemented experimentally. Experimental setup described in Figure 2.4 was considered to implement the control methods. Controller gains were $k = 3.2$; $q = 2.8$ and observer gain was $k_o = 6.5$.

5.7.1 Observer Performance

Here the angular displacement and tip deflection (measured using an encoder and strain gauge respectively) are compared with observer outputs. Figures 5.10 and 5.11 show the estimation error results for SMO and Figures 5.12 and 5.13 show the estimation error results for FSMO.

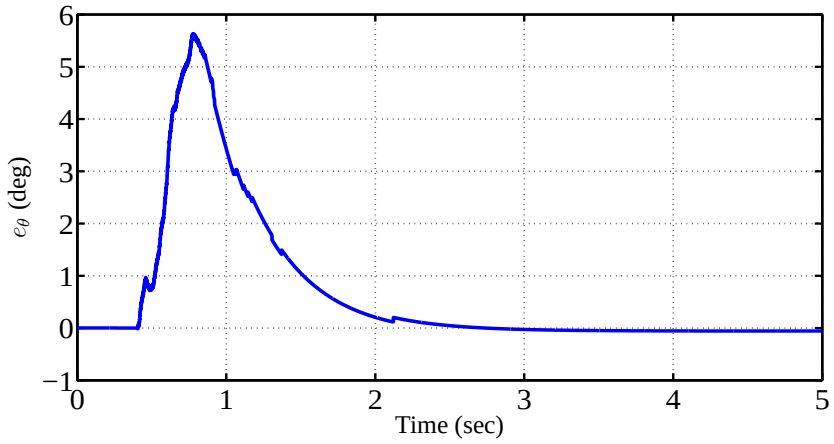

Figure 5.10: SMO: Estimation error in θ

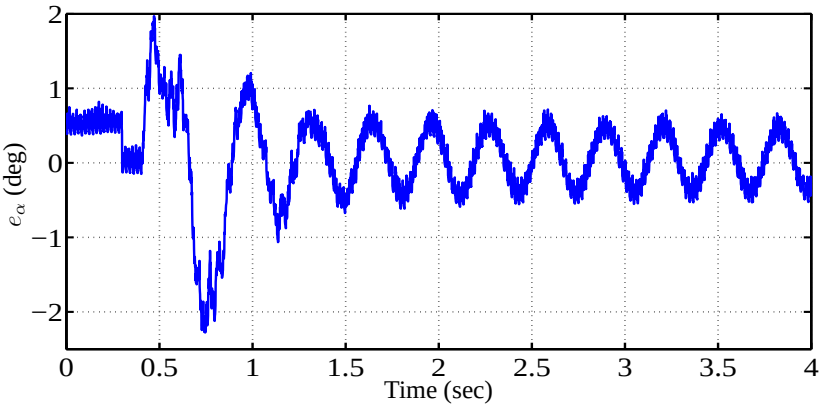

Figure 5.11: SMO: Estimation error in α

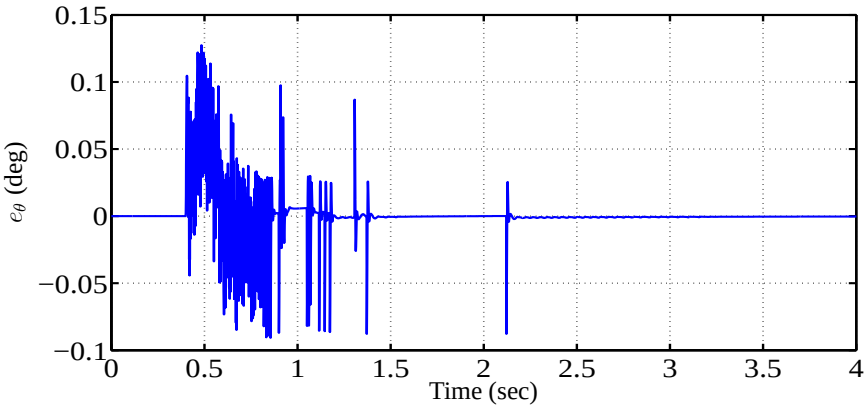

Figure 5.12: FSMO: Estimation error in θ

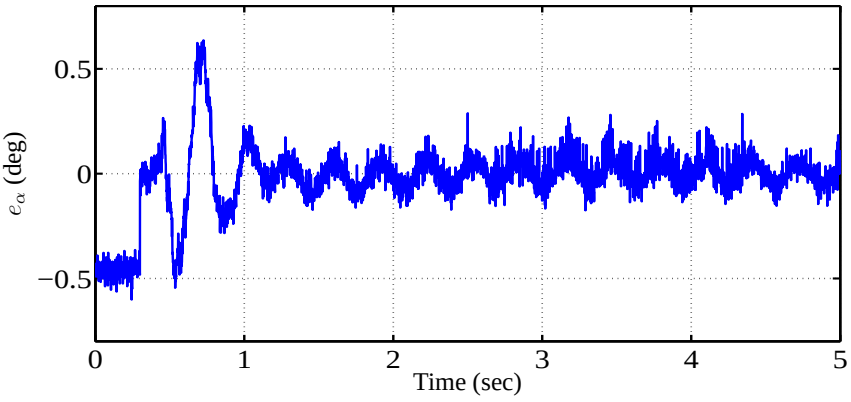

Figure 5.13: FSMO: Estimation error in α

It can be observed that the sliding mode dynamics force the output estimation error to zero in finite time. The strain gauge sensor used for angular tip displacement has a significant error which results in a noisy output.

5.7.2 Controller Performance

Figure 5.14 and 5.15 show the evolution of all states experimentally and Figure 5.16 shows the control input.

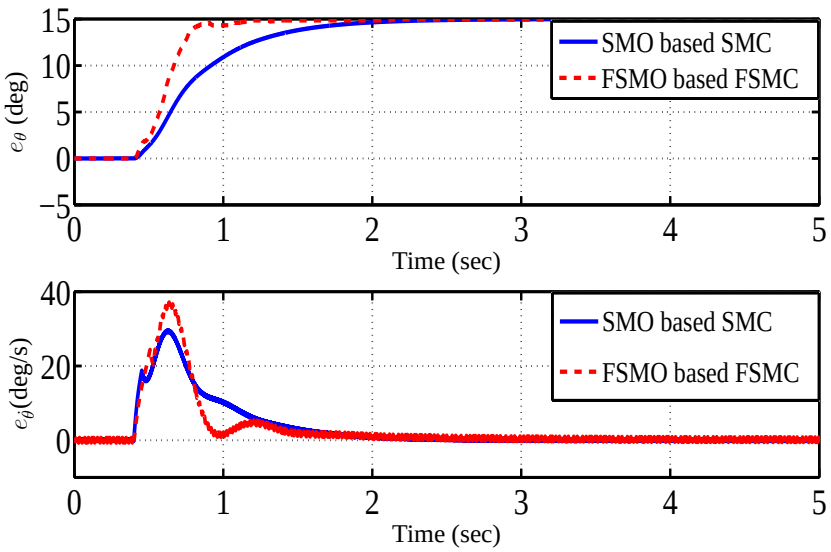

Figure 5.14: Evolution of output angular displacement and its rate

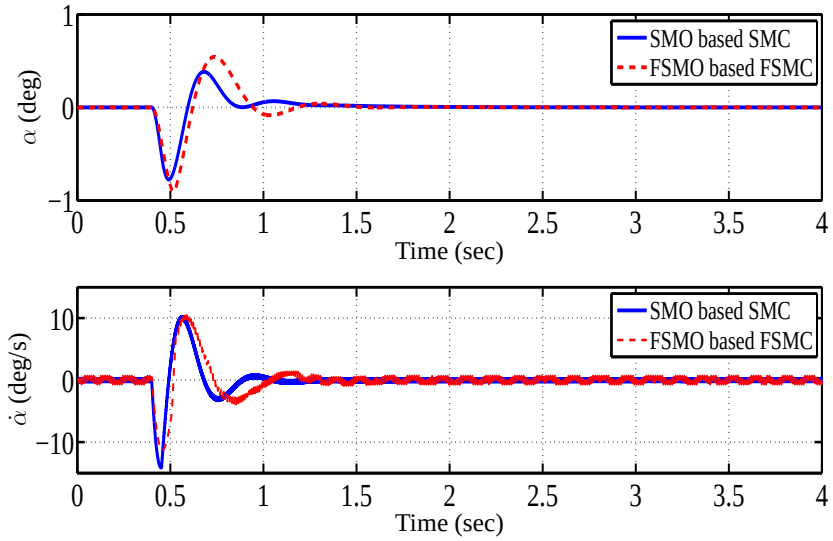

Figure 5.15: Evolution of angular tip displacement and its rate

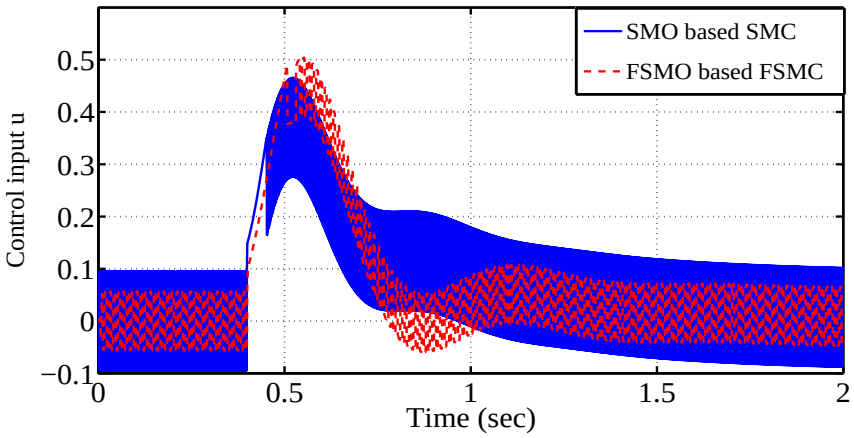

Figure 5.16: Control Input

Strategy	$\|u\|_2$	$\|u\|_\infty$	$\|\theta\|_1$	$\|\alpha\|_1$
SMC with SMO	14.4469	0.79	72153	189.34
FSMC with FSMO	9.7845	0.70	71987	170.88

Table 5.2: Comparison of performance for SMC and FSMC in experimentation

It can be seen from the plots that for similar performance, FSMC with FSMO results show reduced vibrations and reduced control efforts. Tip vibrations are seen to be reduced

by around 10% using FSMC with FSMO scheme compared to SMC with SMO. The control efforts are reduced by 11%. This analysis is tabulated in Table 5.2. The experimental results show better performance of FSMC with FSMO than the integer order sliding schemes. Control quality of FSMC with FSMO is 32.27% better than that of SMC with SMO. Thus FSMC with FSMO outperforms SMC with SMO.

5.8 Summary

Non-commensurate fractional order model has been developed for SLFM. Superiority of the fractional model w.r.t. IO model has been verified by experimental validation. A novel,stable fractional sliding surface was designed. Control was synthesized using fractional reaching law. FSMO provides Estimates of fractional states for implementing controller. FSMO provided fast converging estimates of states. Performance of FSMC based FSMO to achieve positional accuracy of SLFM with minimum vibrations has been verified. FSMC with FSMO yielded superior performance compared to SMC with SMO. The method of FSMC with FSMO can be extended to any second order under actuated system of this class.